AD_____

Award Number: W81XWH-04-1-0330

TITLE: Optical Spectroscopy and Multiphoton Imaging for the Diagnosis and Characterization of Hyperplasias in the Mouse Mammary Gland

PRINCIPAL INVESTIGATOR: Melissa Caroline Skala

CONTRACTING ORGANIZATION: University of Wisconsin
Madison, WI 53706

REPORT DATE: September 2005

TYPE OF REPORT: Annual Summary

PREPARED FOR: U.S. Army Medical Research and Materiel Command
Fort Detrick, Maryland 21702-5012

REPORT DOCUMENTATION PAGE

Form Approved
OMB No. 0704-0188

1. REPORT DATE	2. REPORT TYPE	3. DATES COVERED
01-09-2005	Annual Summary	1 Sep 2004 – 30 Aug 2005

4. TITLE AND SUBTITLE

Optical Spectroscopy and Multiphoton Imaging for the Diagnosis and Characterization of Hyperplasias in the Mouse Mammary Gland

5a. CONTRACT NUMBER

5b. GRANT NUMBER
W81XWH-04-1-0330

5c. PROGRAM ELEMENT NUMBER

6. AUTHOR(S)

Melissa Caroline Skala

5d. PROJECT NUMBER

5e. TASK NUMBER

5f. WORK UNIT NUMBER

7. PERFORMING ORGANIZATION NAME(S) AND ADDRESS(ES)

University of Wisconsin
Madison, WI 53706

8. PERFORMING ORGANIZATION REPORT NUMBER

9. SPONSORING / MONITORING AGENCY NAME(S) AND ADDRESS(ES)
U.S. Army Medical Research and Materiel Command
Fort Detrick, Maryland 21702-5012

10. SPONSOR/MONITOR'S ACRONYM(S)

11. SPONSOR/MONITOR'S REPORT NUMBER(S)

12. DISTRIBUTION / AVAILABILITY STATEMENT
Approved for Public Release; Distribution Unlimited

13. SUPPLEMENTARY NOTES

14. ABSTRACT

There is no reliable method for identifying pre- or non-malignant lesions in animal models of breast cancer *in vivo* and thus no method for studying carcinogenesis *in vivo*. The purpose of this project is to develop a method to diagnose mammary gland hyperplasias in an animal model *in vivo* using optical spectroscopy. The absorption and scattering parameters extracted from diffuse reflectance spectra measured *in vivo* in the 400-600 nm range were used to differentiate normal tissue (n=23) and benign lesions (n=16) of the exposed mammary glands of 17 ENU-treated FVBxB6 *Apc*$^{Min/+}$ mice. Malignant lesions (n=3) were identified by palpation. Wilcoxon rank sum tests revealed a statistically significant increase ($p<0.05$) in total hemoglobin concentration for benign lesions compared to the normal mammary gland. Statistically significant differences ($p<0.05$) in the mean reduced scattering coefficient were also found between two sub-classes of benign lesions. Subsequent studies will focus on the differentiation of normal and malignant lesions. In the future, this technique could be used to noninvasively determine which benign lesions ultimately become malignant. This has important implications for longitudinal disease progression

15. SUBJECT TERMS
diagnosis, fluorescence, hyperplasia, mouse, multiphoton microscopy, Spectroscopy statistical algorithm

16. SECURITY CLASSIFICATION OF:			17. LIMITATION OF ABSTRACT	18. NUMBER OF PAGES	19a. NAME OF RESPONSIBLE PERSON
a. REPORT	b. ABSTRACT	c. THIS PAGE			USAMRMC
U	U	U	UU	34	19b. TELEPHONE NUMBER *(include area code)*

Table of Contents

Introduction

The purpose of this project is to develop a method to diagnose mammary gland hyperplasias in an animal model *in vivo* using optical spectroscopy. If successful, the outcomes of this project could lead to the design of an optically based system for *in vivo* diagnosis of mammary gland tumors and hyperplasias, thus allowing research of the hyperplasia-tumor sequence in an animal model. The specific objectives are to measure the optical spectra of tumors, hyperplasias and normal tissues in the mouse mammary gland and to quantitatively identify the optical spectral variables that show the greatest contrast between tumors, hyperplasias and normal tissues in the mouse mammary gland. Physiological parameters extracted from measured optical spectra will be verified independently with electrode measurements of pO_2 in carcinomas and normal regions of the mammary gland.

Body

Fluorescence and diffuse reflectance spectra have been measured in 17 ethylnitrosourea (ENU) treated mice *in vivo* (Task 1, parts (a) and (b)). Histological analysis of the measured sites in the mammary gland confirm n=23 normal tissue sites, n=16 hyperplastic sites and n=3 carcinomas (Task 1, part (d)). All of the carcinomas were palpable and none of the hyperplastic lesions were palpable. The variability in normal mammary glands will be evaluated with the measurements from normal regions of these ENU-treated mice (Task 1, part (c)). This work addresses Task 1 in the statement of work.

Meaningful physiological parameters, including total hemoglobin concentration, hemoglobin saturation and tissue scattering have been extracted from the measured

diffuse reflectance spectra. Differences in these physiological parameters between histologically confirmed normal and hyperplastic regions of the mammary gland were evaluated with non-parametric Wilcoxon rank sum tests. There was a statistically significant increase ($p<0.05$) in total hemoglobin concentration for hyperplasia compared to the normal mammary gland. Hyperplastic lesions were further sub-divided as small mammary tumors (SMT) or focal alveolar hyperplasia (FAH) based on their morphological appearance under whole mount. Statistically significant differences ($p<0.05$) in the mean reduced scattering coefficient were found between these two gross sub-classes of hyperplasias. A manuscript detailing these results and their implications has been submitted to the peer-reviewed journal, *Lasers in Surgery and Medicine*, and is included in Appendix A. This work addresses Task 2 (a) for the normal vs. hyperplasia comparison, and Task 2 (c). The fiber optic probe used in this study had a single source-detector separation, so it was not necessary to identify an optimal source-detector separation (Task 2 (b)). Due to the small sample size, statistical tests were not performed on the carcinomas (n=3). The normal vs. carcinoma comparison for Task 2 (a) will be completed in conjunction with Task 3. In Task 3, electrode measurements of pO_2 will be used to verify tissue oxygenation extracted from measured diffuse reflectance spectra of rat mammary carcinomas. This third task will be completed at Duke University, where the PI and her advisor have transferred for the remainder of the PI's PhD (PI's start date at Duke University is August, 2005).

Key Research Accomplishments

- Measured fluorescence and diffuse reflectance of ethylnitrosourea (ENU) treated mouse mammary glands over the entire ultraviolet to visible (UV-VIS) wavelength range *in vivo*.

- Quantitatively identified the optical spectral variables that show the greatest contrast between hyperplasias and normal regions of the mouse mammary gland.

- Quantitatively identified the optical spectral variables that show the greatest contrast between sub-groups of mammary gland hyperplasias

Reportable Outcomes

Journal Articles:

- Melissa C. Skala, Gregory M. Palmer, Benjamin J. Sprague, Ruth Sullivan, Amy R. Moser, Nirmala Ramanujam. "Optical Properties of Benign Lesions of the Mouse Mammary Gland." Submitted, Lasers Surg Med.

Conference Presentations:

- Melissa C. Skala, Gregory M. Palmer, Benjamin J. Sprague, Ruth Sullivan, Amy R. Moser, Nirmala Ramanujam. Optical Properties Differentiate Normal, Malignant and Non-Malignant Lesions in the Mouse Mammary Gland. Era of Hope Meeting (Department of Defense Breast Cancer Research Program), 2005. Philadelphia, PA.

Training Accomplishments

Degrees Obtained:

- Master of Science, Biomedical Engineering, May 2004

Awards:

- American Society for Laser Medicine and Surgery competitive summer research grant, 2004
- American Society for Laser Medicine and Surgery national meeting competitive travel grant, 2004

Conclusions

Normal and hyperplastic regions of the mouse mammary gland have been differentiated *in vivo* with optical spectroscopy. Two different sub-classes of hyperplasias have also been differentiated with optical spectroscopy *in vivo*. At present we do not know if these

two classes of hyperplasias represent stages of progression from hyperplasia to malignancy, or whether they represent two different types of benign lesions. However, this preliminary study (see Appendix A) indicates that optical spectroscopy could be used to follow the two classes of hyperplasias in the mammary gland *in vivo* over time to determine whether the lesions remain benign or become malignant. Time course experiments will allow for a greater understanding of disease progression in animal models of breast cancer. The physical features used to differentiate mouse mammary lesions in this study may offer insight into the biological basis for the difference between normal and non-malignant lesions. Future studies will investigate the optical contrast between normal and malignant lesions in animal models of breast cancer *in vivo* (remainder of Task 2). Optical methods for measuring tissue oxygenation will also be verified with electrode measurements of pO_2 in the normal and malignant rat mammary gland (Task 3).

References

Melissa C. Skala, Gregory M. Palmer, Benjamin J. Sprague, Ruth Sullivan, Amy R. Moser, Nirmala Ramanujam. "Optical Properties of Benign Lesions of the Mouse Mammary Gland." Submitted, Lasers Surg Med.

Optical Properties of Benign Lesions in the Mouse Mammary Gland

Melissa C. Skala, MS[1*], Gregory M. Palmer, MS[1*], Benjamin J. Sprague[1,2], Ruth Sullivan, VMD, PhD[3], Amy R. Moser, PhD[2], Nirmala Ramanujam, PhD[1*]

[1]Department of Biomedical Engineering, University of Wisconsin, Madison, WI 53706
[2]Department of Human Oncology, University of Wisconsin, Madison, WI 53792
[3]Comprehensive Cancer Center and Waisman Center, University of Wisconsin, Madison, WI 53705

*Current Address: Department of Biomedical Engineering, Duke University, Durham, NC, 27708

Funding: DOD W81XWH-04-1-0330

For Correspondence
Nirmala Ramanujam
Duke University
Department of Biomedical Engineering
136 Hudson Hall
Box 90281, Campus
Durham, NC 27708-0281
Phone: 919-660-5307
Fax: 919-684-4488
Email: nimmi@duke.edu

Keywords: absorption, diagnosis, diffuse reflectance spectroscopy, hemoglobin concentration, hyperplasia, in vivo, oxygen saturation, scattering, UV-VIS

Abbreviations: SMT – small mammary tumor, FAH – focal alveolar hyperplasia

Abstract

Background and Objective: There is a need for noninvasive, non-toxic methods to study tumor progression and treatment in animal models. Malignant tumors in the widely used $Apc^{Min/+}$ model of breast cancer can be detected by palpation, but there is no reliable method for identifying pre- or non-malignant lesions in the mammary gland *in vivo* and thus no method for studying carcinogenesis *in vivo* in this model. Diffuse reflectance spectroscopy is promising for the detection of lesions in the mammary gland *in vivo* because it is sensitive to the intrinsic physiology and structure of tissue, including total hemoglobin concentration, hemoglobin saturation and tissue scattering. **Study Design/Materials and Methods:** The absorption and scattering parameters extracted from diffuse reflectance spectra measured *in vivo* in the 400-600 nm range were used to differentiate normal tissue (n=23) and benign lesions (n=16) of the exposed mammary glands of 17 ENU-treated FVBxB6 $Apc^{Min/+}$ mice. Malignant lesions were identified by palpation. **Results:** Wilcoxon rank sum tests revealed a statistically significant increase ($p<0.05$) in total hemoglobin concentration for benign lesions compared to the normal mammary gland. Statistically significant differences ($p<0.05$) in the mean reduced scattering coefficient were also found between two sub-classes of benign lesions (focal alveolar hyperplasias and small mammary tumors). **Conclusions:** This preliminary study indicates that normal and benign lesions, and sub-classes of benign lesions in the mouse mammary gland can be differentiated with optical spectroscopy *in vivo* based on endogenous physiological and structural parameters. In the future, this technique could be used to identify benign lesions before they become palpable, and thus provide a means

of identifying which benign lesions ultimately become malignant. This has important implications for longitudinal disease progression studies.

Introduction

Animal models are widely used for studying tumor progression and treatment. Currently, animal studies of tumor progression require either (1) euthanizing animals at multiple time points during tumor progression, or (2) transplanting lesions at multiple stages of tumor progression into host animals. Both of these techniques require large numbers of animals. In the first type of experiment, the developmental fate of each lesion cannot be determined, but must be extrapolated from lesions at later time points. The second type of experiment assumes that transplantation will have no effect on the progression of lesions. The study of tumor progression in intact animals will allow the developmental fate for all lesions to be known, without introducing perturbations that could alter the behavior of lesions.

Mutations in the *Apc* (adenomatous polyposis coli) tumor suppressor gene predispose mice and humans to the development of several tumor types. The widely used $Apc^{Min/+}$ female mouse model (1,2) develops hyperplasias and malignant lesions in the mammary gland after a single injection with ethylnitrosourea (ENU), a direct-acting mutagen (3). Each mouse develops multiple lesions, some of which may be malignant. The tumors are either squamous cell carcinomas or adenocarcinomas. It is currently not clear which of the pre-malignant lesions progress to malignancy, and which remain benign. To understand the mechanisms that create malignant lesions in this model, it is necessary to follow the lesions to their endpoints.

Malignant tumors in the $Apc^{Min/+}$ model can be detected by palpation, but there is currently no reliable method for identifying pre- or non-malignant lesions in the mammary gland *in vivo*. Thus, it is difficult to determine the fate of these lesions, i.,e.,

which ones become malignant. A method to detect pre-malignant and non-malignant lesions *in vivo* is needed to determine which lesions progress to malignancy and which remain benign. Ideally, detection would not require exogenous contrast agents that could alter the biology of the lesions, and would be non-invasive and non-toxic to allow for repeated evaluations.

Diffuse reflectance spectroscopy in the ultraviolet-visible (UV-VIS) wavelength range is promising for the detection of pre-/non-malignant lesions in the mammary gland *in vivo* because it is sensitive to the intrinsic physiology and structure of tissue (4,5). Previous studies have investigated the use of diffuse reflectance spectroscopy for the diagnosis of breast cancer in humans, yet few have investigated animal models of breast cancer *in vivo*. In this study, an inverse Monte Carlo based model (6) will be used to extract physiologically meaningful parameters from diffuse reflectance spectra measured *in vivo*, including total hemoglobin concentration, hemoglobin oxygen saturation and tissue scattering. The goal of this study is to differentiate normal and benign (pre- and non-malignant) lesions *in vivo* in the mouse mammary gland with these physiological and structural parameters. Non-invasively identifying benign lesions in the mouse mammary gland with a fast optical technique will potentially enable the discrimination between benign lesions that become malignant, and benign lesions that remain non-malignant.

Materials and Methods

ENU-Treated Mouse Mammary Gland Model of Breast Cancer

A total of 17 ENU-treated mice were evaluated in this study. Female F1 FVB/NTac x C57BL6/J (FVBXB6) $Apc^{Min/+}$ mice were generated by crossing FVB females with B6 $Apc^{Min/+}$ male mice. The $Apc^{Min/+}$ female offspring were given a single intraperitoneal injection of ENU (50mg/kg body weight) when between 35 and 40 days of age (3). The mice were then palpated weekly for the presence of tumors. When a tumor was identified or the mouse reached 9 months of age, the mouse was entered into the study. Animal care and procedures were in accordance with the guidelines in the U.S. Department of Health and Human Services and National Institutes of Health "Guide for the Care and Use of Laboratory Animals" and approved by the Institutional Animal Care and Use Committee at the University of Wisconsin.

Instrumentation

All measurements were made using a Skinscan spectrofluorometer (JY Horiba, Edison, NJ). This instrument consists of a 150 W xenon lamp, double grating excitation and emission monochromators having fixed bandpasses of 5 nm for both excitation and emission, and a photomultiplier tube (PMT). The adjustable parameters of the system are the wavelength range and increment, the signal acquisition time and the PMT high voltage. The illumination and collection of light was coupled through a fiber optic probe, consisting of a central collection core with a diameter of 1.52 mm surrounded by an illumination ring, with an outer diameter of 2.18 mm. Both the illumination ring and collection core are made up of 31 individual fibers, each with a core/cladding diameter of

200/245 μm. The numerical aperture of the excitation and emission fibers is 0.125 and 0.12, respectively.

Simulations using a modified, three-dimensional, weighted-photon Monte Carlo code have been carried out to evaluate the probing depth achieved with this illumination and collection geometry in a turbid medium (7). For a homogeneous medium with a fixed scattering coefficient of 110.4 cm^{-1}, and absorption coefficient varying from 31.8 cm^{-1} to 1.3 cm^{-1} (i.e., absorption coefficients spanning the UV-VIS range), the probing depth varied from 450 to 1350 μm. In a turbid medium with a fixed absorption coefficient of 10.8 cm^{-1}, and scattering coefficient varying from 225 cm^{-1} to 50 cm^{-1} (i.e., scattering coefficients spanning the UV-VIS range), the probing depth varied from 550 to 1050 μm. The probing depth in a medium with absorption (2.3 cm^{-1}) and scattering coefficients (167 cm^{-1}) representative of breast adipose tissue at 540 nm (8) was 1050 μm. The mammary fat pads were generally greater than 3 mm in thickness, and thus could be considered a semi-infinite medium for this particular probe geometry.

Diffuse Reflectance of Mouse Mammary Gland in vivo

Diffuse reflectance spectra were collected from 42 mouse mammary gland sites in a total of 17 mice. Mice were anesthetized with a gas anesthesia machine (Tech IV isoflurane vaporizer, Surgivet). Mice were initially ventilated with 3% isoflurane, and after the animal was sedated the isoflurane was maintained at 1 to 2%. A subset of the lesions was identified by palpation. Next, the gland(s) were exposed by inverting the overlying skin. Lesions that were identified by palpation were confirmed by visual inspection of the exposed gland (3). Potential lesions were identified by visual inspection once the

mammary glands were exposed. However, since lesions are generally not identifiable by visual inspection alone, diffuse reflectance spectra were measured from several random sites in the mammary gland to increase the likelihood that a lesion is sampled. The probe was placed flush against the tissue surface and secured into place with a clamp assembly prior to the measurement.

Diffuse reflectance was measured from 300 to 900 nm. This measurement was made in a synchronous scan mode, whereby the excitation and emission gratings are moved simultaneously. The diffuse reflectance measurements were made at an increment of 5 nm, with a signal acquisition time of 0.1s/wavelength and at a PMT high voltage of 370 V. The diffuse reflectance spectrum was corrected for the wavelength-dependent system response and the throughput of the instrument by normalizing it to that of a Spectralon 99% reflectance puck (SRS-99–010, Labsphere, Inc., North Sutton, NH), which was measured with the probe in contact with the puck (no coupling media was used). After each diffuse reflectance measurement, the measured site was marked on the surface of the gland with pathology ink. The animal was euthanized with carbon dioxide (CO_2) inhalation after all sites of interest had been measured.

Whole Mount and Histopathology Analysis of the Mouse Mammary Gland

After the animals were euthanized, the mammary fat pads were collected and processed for whole mount staining (3). After staining, the whole mounts were assessed to classify the regions scanned as either normal or hyperplastic, photographed, and the hyperplastic lesions were measured and collected for histological processing. Malignant lesions were excised and sent for histological processing without whole mount stain. Hyperplastic lesions were classified as small mammary tumors (SMT) or focal alveolar hyperplasia

(FAH) based on their morphological appearance in the whole mount stains. Histological sections of hyperplastic and malignant lesions were evaluated by a pathologist who had no prior knowledge of the classification based on the whole mount appearance.

Figure 1 shows a flowchart for the identification and classification of lesions in the mouse mammary gland. The entire mammary gland was evaluated by visual inspection *in vivo*, to identify potential sites of interest for optical measurements. The entire lesion was evaluated by whole mount stain in the intact mammary gland *ex vivo* to classify benign lesions based on the lesion size and macroscopic morphology. Microscopic samples of the lesion were evaluated by histopathology to diagnose lesions as either benign or malignant based on cellular-level morphology. The complimentary information from whole mount stain and histopathology allows for both macroscopic and microscopic lesion features to be classified, respectively.

Analysis of Diffuse Reflectance

The Monte Carlo inverse model was used to extract the absorption and scattering coefficients from the measured diffuse reflectance spectra and this model is described in detail in a previous paper (6). The fixed parameters of the model are the absorbers assumed to be present in the biological system, the extinction coefficient of the absorbers and the refractive index mismatch between the scatterer and the surrounding medium. The free parameters of the model are the concentration of absorbers, the scatterer size and scatterer density. A non-linear least squares optimization algorithm is used to minimize the difference between the modeled and measured diffuse reflectance spectra, and the free parameters of the best fit are retained. The extracted absorber concentrations and the wavelength dependent extinction coefficients can be used to determine the absorption

coefficient at a given wavelength using Beer's law. The scatterer size, density, wavelength and refractive index mismatch can be used to determine the scattering coefficient at a given wavelength using Mie theory.

First, the model was validated by using it to extract the absorption coefficient and reduced scattering coefficient from known tissue phantoms consisting of water soluble human hemoglobin as an absorber (absorption coefficient ranging from 0-17.5 cm^{-1}) and 1 μm polystyrene spheres as a scatterer (reduced scattering coefficient ranged from 10.9-16.4 cm^{-1}). The model extracted the absorption coefficient and the reduced scattering coefficient with an error of 3.1 ± 1.1% and 2.5 ± 0.7%, respectively in a total of five separate tissue phantoms (6).

Next, the model was used to analyze the diffuse reflectance spectra measured from the mouse mammary gland. The wavelength range of the diffuse reflectance spectrum was restricted to 400-600 nm to simplify the use of the model by reducing the number of absorbers that would have to be accounted for (by excluding proteins and other chromophores that absorb below 400 nm), and to ensure that the tissue could be modeled as a semi-infinite medium (by excluding wavelengths above 600 nm where tissue has very low absorption). The semi-infinite assumption simplifies the model because the depth does not need to be fit as a free parameter.

Prior to the fitting, each tissue diffuse reflectance spectrum was divided (at each wavelength) by the diffuse reflectance spectrum of a reference tissue phantom composed of hemoglobin and polystyrene spheres with known optical properties (mean reduced scattering coefficient of 13 cm^{-1}, mean absorption coefficient of 0 cm^{-1}). The modeled diffuse reflectance spectrum was calibrated in a similar manner, i.e., by dividing the

modeled diffuse reflectance spectrum by that of a reference phantom with the same pre-defined absorption and reduced scattering coefficient range. This accounted for the throughput and the wavelength response of the spectrometer used in these studies, and corrected differences in the magnitude of the Monte Carlo simulations (which are on an absolute scale) and the experimental measurements, which are on a relative scale.

The refractive indices of the scatterers and the surrounding medium were fixed parameters and were assumed to be 1.4 and 1.36, respectively in the inverse model. The effect of this assumption was investigated in a previous study, and found to have a minimal impact upon the accuracy of optical property extraction (6). The free parameters of the fit relating to scattering were the scatterer size and density. The scatterer size was constrained to be between 0.35 and 1.5 μm diameter (4,9-13). The intrinsic chromophores were assumed to be oxygenated and deoxygenated hemoglobin (4,14,15), and their wavelength dependent extinction coefficients (fixed parameters) were obtained from an online database (16). The free parameters of the fit relating to absorption were the concentrations of each absorber.

After the inverse model was applied to the diffuse reflectance spectra to extract the absorption and scattering parameters, a Wilcoxon rank-sum test (17) was then used to determine which extracted features showed statistically significant differences between normal and benign lesions (FAH and SMT) and between the two classes of benign lesions.

Results

Whole Mount and Histopathology Results

A total of 42 tissue sites were measured in this study, of which 23 were normal, 16 were benign and three were malignant based on histopathology. All of the malignant lesions were palpable, and none of the benign lesions were palpable. The malignant tumors were not included in the optical analysis due to the small sample size. The benign lesions were classified as focal alveolar hyperplasias with some squamous metaplasia, based on the histology. The whole mount analysis revealed two sub-classes of benign lesions: FAH (n=7 sites) and SMT (n=9 sites). Figure 2 shows representative (a) whole mount and (b) histology of one normal site, FAH, SMT, and malignant tumor in the mouse mammary gland. The classification of lesions into FAH or SMT was based on the appearance in the whole mount. FAH were generally more diffuse lesions with a clear appearance of alveolar hyperplasia. SMT, although not palpable, resembled the palpable tumors in that they were frequently more clearly defined and appeared more solid than did the lesions classified as FAH. There were also lesions that shared some aspects of both categories and were classified based on which aspects predominated. Sites classified as "normal" had no abnormal lesions within the areas marked by the pathology ink, or close by.

Optical Properties of Normal and Benign Lesions in the Mouse Mammary Gland

Figure 3 shows the diffuse reflectance spectra measured from one (a) normal, and each of the benign lesions (FAH, (b) and SMT, (c)), and the corresponding fit to the inverse Monte Carlo model. The fits appear to agree well with the diffuse reflectance spectra measured from each of the tissue categories.

Figure 4 shows the extracted (a) absorption coefficient and (b) reduced scattering coefficient spectra for the samples shown in Figure 3. All samples have significant hemoglobin absorption (absorption maxima at 420 nm, 540 nm and 580 nm), and the benign lesions have higher hemoglobin absorption than the normal mammary gland (Fig. 4 (a)). The FAH sample also has a higher reduced scattering coefficient at all wavelengths compared to the SMT sample (Fig. 4 (b)).

Figure 5 shows the extracted (a) hemoglobin concentration, (b) hemoglobin saturation, and (c) mean reduced scattering coefficient (averaged over the 400-600 nm wavelength range) averaged for the n=23 normal sites, n=7 FAHs, and n=9 SMTs. The total hemoglobin concentration for FAH and SMT is statistically greater than normal (Fig. 4 (a), $p<0.05$), the hemoglobin saturation for SMT is statistically greater than normal (Fig. 4 (b), $p<0.05$), and the mean reduced scattering coefficient for FAH is statistically greater than SMT (Fig. 4 (c), $p<0.05$). Thus, the benign lesions are differentiated from normal by the total hemoglobin concentration and the two sub-classes of benign lesions are differentiated by the mean reduced scattering coefficient.

Discussion

The results of this preliminary study indicate that normal tissue and benign lesions in the mouse mammary gland can be differentiated *in vivo* with diffuse reflectance spectroscopy. Benign lesions had statistically higher hemoglobin concentrations than normal tissue. In addition, the two different classes of benign lesions could be differentiated *in vivo* with just the mean reduced scattering coefficient. At present we do not know if either or both of these two sub-classes have the potential to become malignant. However, the difference in optical properties between these two distinctly different sub-classes may allow us to identify these lesions well before they become palpable, and thus provide a means of identifying which benign lesions ultimately become malignant.

Future studies will also investigate the optical contrast between benign and malignant lesions in the mouse mammary gland *in vivo* (the current study focused on identifying benign lesions for optical measurements). Differentiating benign from malignant in addition to normal from benign will allow for monitoring disease progression non-invasively in the Apc^{Min} model of breast cancer, and will also be useful for monitoring the effect of therapeutic agents (18,19).

This study demonstrated that it is feasible to differentiate normal and benign lesions (and different types of benign lesions) in the surgically exposed mammary gland. Future studies will explore completely noninvasive optical diagnostic techniques. This could be achieved by using near infrared diffuse optical spectroscopy (20) to probe deeper into tissue and the use of two-layer light transport models to account for the

effects of skin absorption and scattering in the quantification of the mammary tissue optical properties (21).

References

1. van der Houven van Oordt CW, Smits R, Williamson SL, Luz A, Khan PM, Fodde R, van der Eb AJ, Breuer ML. Intestinal and extra-intestinal tumor multiplicities in the Apc1638N mouse model after exposure to X-rays. Carcinogenesis 1997; 18(11):2197-2203.
2. Moser AR, Mattes EM, Dove WF, Lindstrom MJ, Haag JD, Gould MN. ApcMin, a mutation in the murine Apc gene, predisposes to mammary carcinomas and focal alveolar hyperplasias. Proc Natl Acad Sci U S A 1993; 90(19):8977-8981.
3. Moser AR, Hegge LF, Cardiff RD. Genetic background affects susceptibility to mammary hyperplasias and carcinomas in Apc(min)/+ mice. Cancer Res 2001; 61(8):3480-3485.
4. Palmer GM, Zhu C, Breslin TM, Xu F, Gilchrist KW, Ramanujam N. A Monte Carlo based inverse model for calculating tissue optical properties, part II: application to breast cancer diagnosis. Appl Opt 2005; Submitted.
5. Ghosh N, Mohanty SK, Majumder SK, Gupta PK. Measurement of optical transport properties of normal and malignant human breast tissue. Applied Optics 2001; 40(1):176-184.
6. Palmer GM, Ramanujam N. A Monte Carlo based inverse model of diffuse reflectance, part I: theory and validation with phantoms. Appl Opt 2005; Accepted.
7. Liu Q, Zhu C, Ramanujam N. Experimental validation of Monte Carlo modeling of fluorescence in tissues in the UV-visible spectrum. J Biomed Opt 2003; 8(2):223-236.
8. Welch JA, Van Gemert CM. Optical-Thermal Response of Laser-Irradiated Tissue. New York: Plenurn. 1995.
9. Mourant JR, Freyer JP, Hielscher AH, Eick AA, Shen A, Johnson TM. Mechanisms of light scattering from biological cells relevant to noninvasive optical-tissue diagnostics. Applied Optics 1998; 37(16):3586-3593.
10. Bolin FP, Preuss LE, Taylor RC, Ference RJ. Refractive index of some mammalian tissues using a fiber optic cladding method. Applied Optics 1989; 28(12):2297-2303.
11. Duck FA. Physical Properties of Tissue: A Comprehensive Reference Book. London: Academic. 1990.
12. Zonios G, Perelman LT, Backman V, Manoharan R, Fitzmaurice M, Van Dam J, Feld MS. Diffuse reflectance spectroscopy of human adenomatous colon polyps in vivo. Applied Optics 1999; 38(31):6628-6637.
13. Mourant JR, Johnson TM, Freyer JP. Characterizing mammalian cells and cell phantoms by polarized backscattering fiber-optic measurements. Applied Optics 2001; 40(28):5114-5123.
14. Yang Y, Celmer EJ, Koutcher JA, Alfano RR. DNA and protein changes caused by disease in human breast tissues probed by the Kubelka-Munk spectral functional. Photochem Photobiol 2002; 75(6):627-632.
15. Palmer GM, Zhu C, Breslin TM, Xu F, Gilchrist KW, Ramanujam N. Comparison of multiexcitation fluorescence and diffuse reflectance spectroscopy for the

diagnosis of breast cancer (March 2003). IEEE Trans Biomed Eng 2003; 50(11):1233-1242.
16. Prahl S. Optical Properties Spectra. Oregon Medical Laser Center 2003 http://omlc.ogi.edu/spectra.
17. Gibbons J, Chakraborti S. Nonparametric Statistical Inference. New York: Marcel Dekker. 1992.
18. Pogue BW, Braun RD, Lanzen JL, Erickson C, Dewhirst MW. Analysis of the heterogeneity of pO2 dynamics during photodynamic therapy with verteporfin. Photochem Photobiol 2001; 74(5):700-706.
19. Kirkpatrick JP, Cardenas-Navia LI, Dewhirst MW. Predicting the effect of temporal variations in PO2 on tumor radiosensitivity. Int J Radiat Oncol Biol Phys 2004; 59(3):822-833.
20. Tromberg BJ, Coquoz O, Fishkin JB, Pham T, Anderson ER, Butler J, Cahn M, Gross JD, Venugopalan V, Pham D. Non-invasive measurements of breast tissue optical properties using frequency-domain photon migration. Philos Trans R Soc Lond B Biol Sci 1997; 352(1354):661-668.
21. Kienle A, Glanzmann T. In vivo determination of the optical properties of muscle with time-resolved reflectance using a layered model. Phys Med Biol 1999; 44(11):2689-2702.

Figure Legends

Figure 1: Flowchart for the identification and classification of lesions in the mouse mammary gland. Potential lesions were first identified by visual inspection of the mammary gland, and sub-classes of benign lesions were identified from whole mount analysis of the entire lesion structure. Histopathology of microscopic sections of the lesion was used to classify benign and malignant lesions.

Figure 2: Whole mount images (a) and histology sections (b) from normal, non-malignant (FAH and SMT) and malignant lesions in the mouse mammary gland. FAH and SMT classification was based on gross inspection of the whole mount. All whole mount images are at the same magnification (7x) and all histology images are at the same magnification (40x). Arrows point to measured sites, which were marked with yellow pathology ink (ink not visible in all images due to conversion to black and white).

Figure 3: Diffuse reflectance spectra for normal (a) and non-malignant lesions (FAH (b) and SMT (c)) measured in the mouse mammary gland *in vivo* and the corresponding fit to the inverse Monte Carlo model. The abbreviation c.u. refers to calibrated units.

Figure 4: The (a) absorption coefficient and (b) reduced scattering coefficient spectra extracted from fits to the diffuse reflectance spectra of the normal tissue sample, FAH and SMT shown in Figure 3.

Figure 5: Extracted values for (a) total hemoglobin concentration, (b) hemoglobin saturation and (c) mean reduced scattering coefficient (averaged over the 400-600 nm wavelength range) for normal and non-malignant lesions (FAH and SMT) in the mouse mammary gland. In the boxplots, the box represents the middle 50% of the measurements (the range of the middle 50% of the data is the interquartile range, IQR), the line through the box represents the median of the measurements and the whiskers extend from the box out through all values that are within 1.5 IQRs of the box. Values that are more than 1.5 IQRs away from the box are outliers, and are indicated separately by circles (17). Unpaired Wilcoxon rank sum tests revealed statistically significant differences ($p<0.05$) in the total hemoglobin concentration of normal vs. FAH and normal vs. SMT (Fig. 4 (a)), in the hemoglobin saturation for normal vs. SMT (Fig. 4 (b)), and in mean reduced scattering coefficient for FAH vs. SMT (Fig. 4 (c)). μ_s' = reduced scattering coefficient.

Figure 1

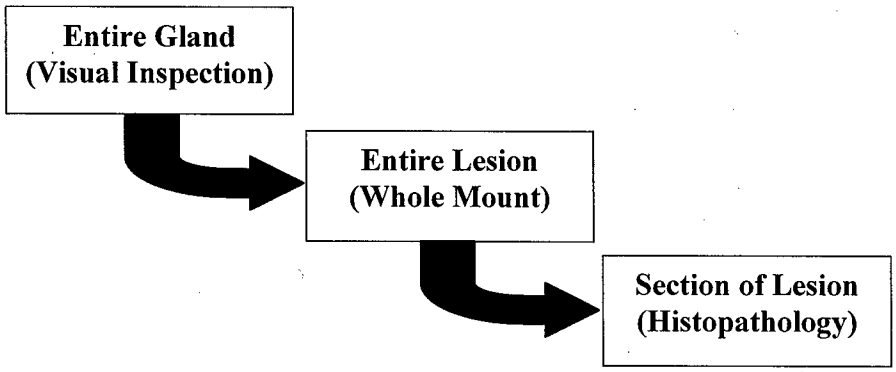
Entire Gland
(Visual Inspection)
Entire Lesion
(Whole Mount)
Section of Lesion
(Histopathology)

Figure 2

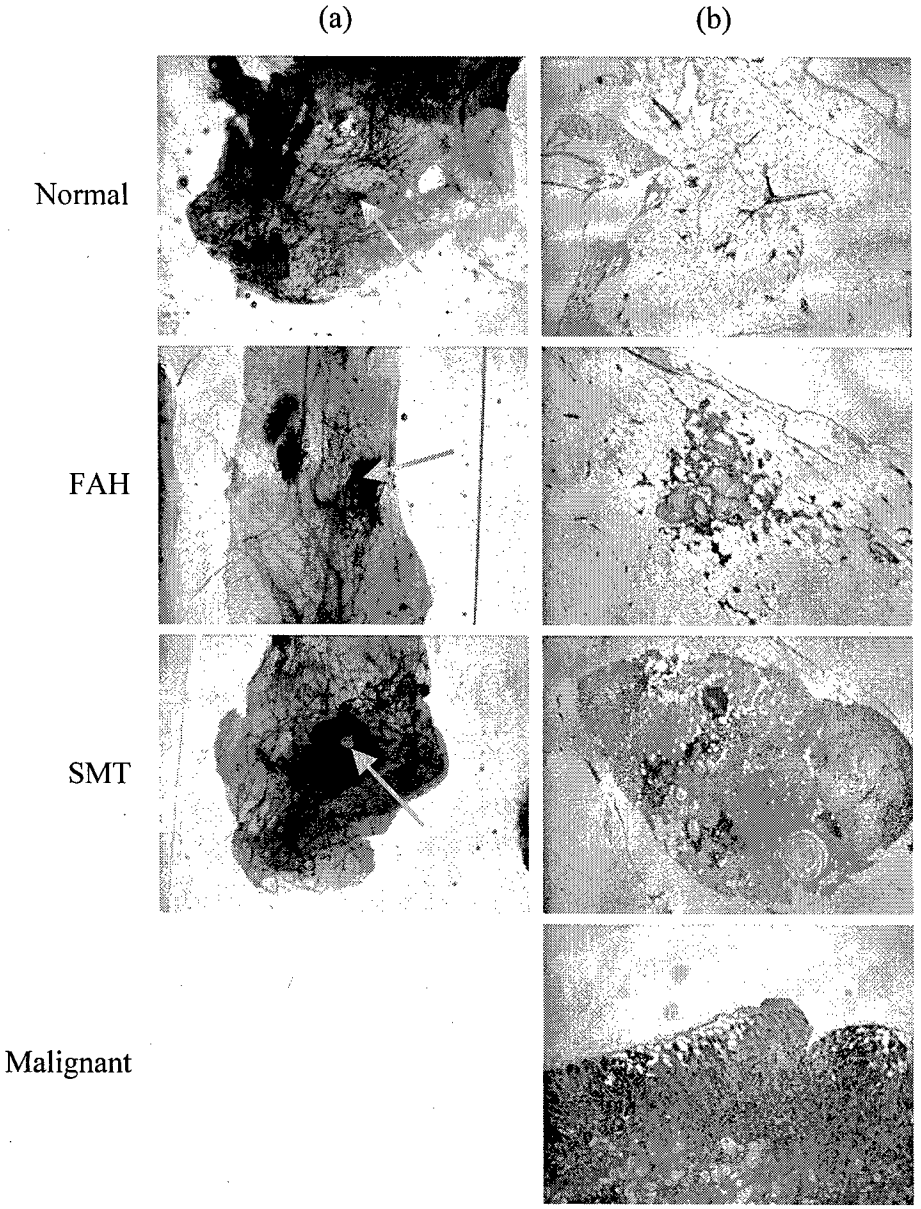

Figure 3

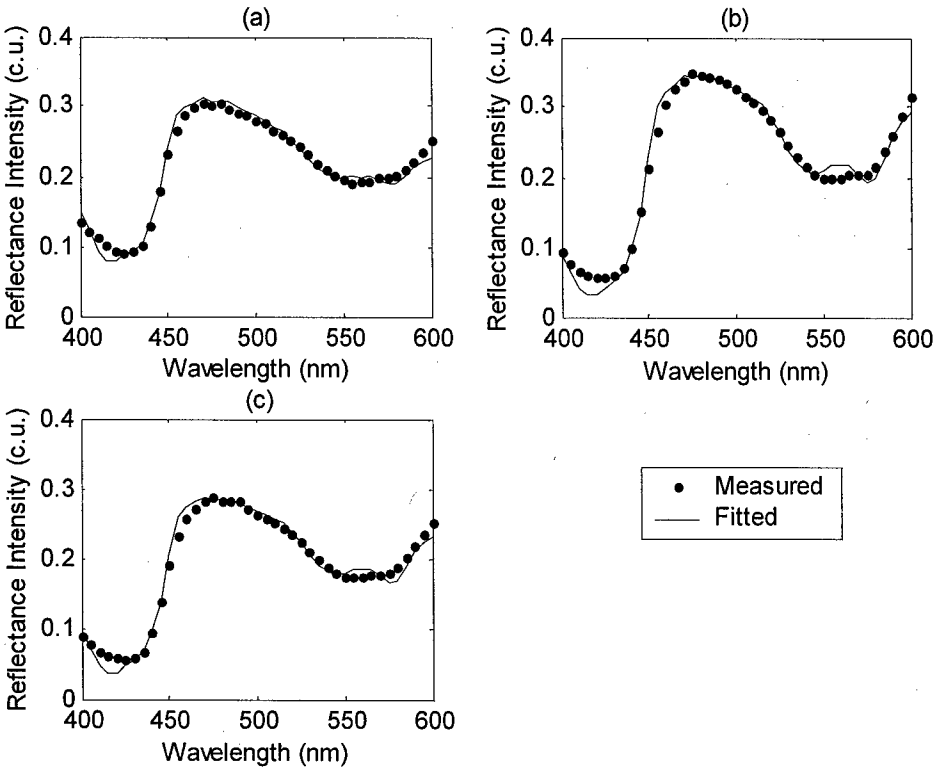
(a)
(b)
(c)
Reflectance Intensity (c.u.)
Wavelength (nm)
0
0.1
0.2
0.3
0.4
400
450
500
550
600
Measured
Fitted

Figure 4 (a)

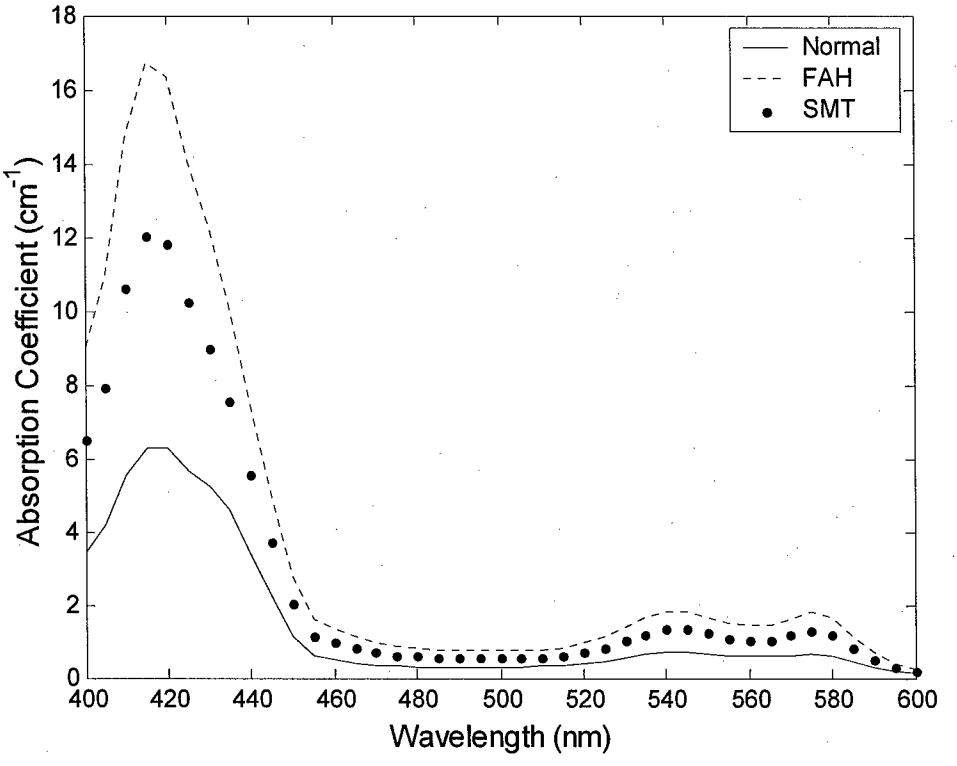
Normal
FAH
SMT
Absorption Coefficient (cm-1)
Wavelength (nm)
0
2
4
6
8
10
12
14
16
18
400
420
440
460
480
500
520
540
560
580
600

Figure 4 (b)

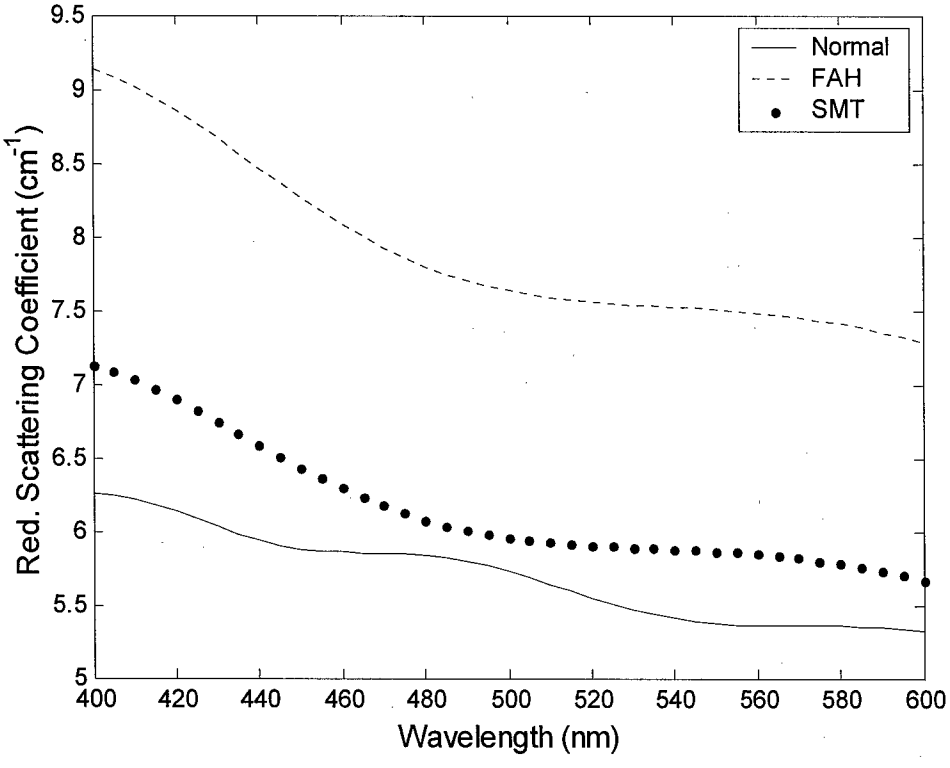
Normal
FAH
SMT
Red. Scattering Coefficient (cm-1)
Wavelength (nm)
9.5
9
8.5
8
7.5
7
6.5
6
5.5
5
400
420
440
460
480
500
520
540
560
580
600

Figure 5 (a)

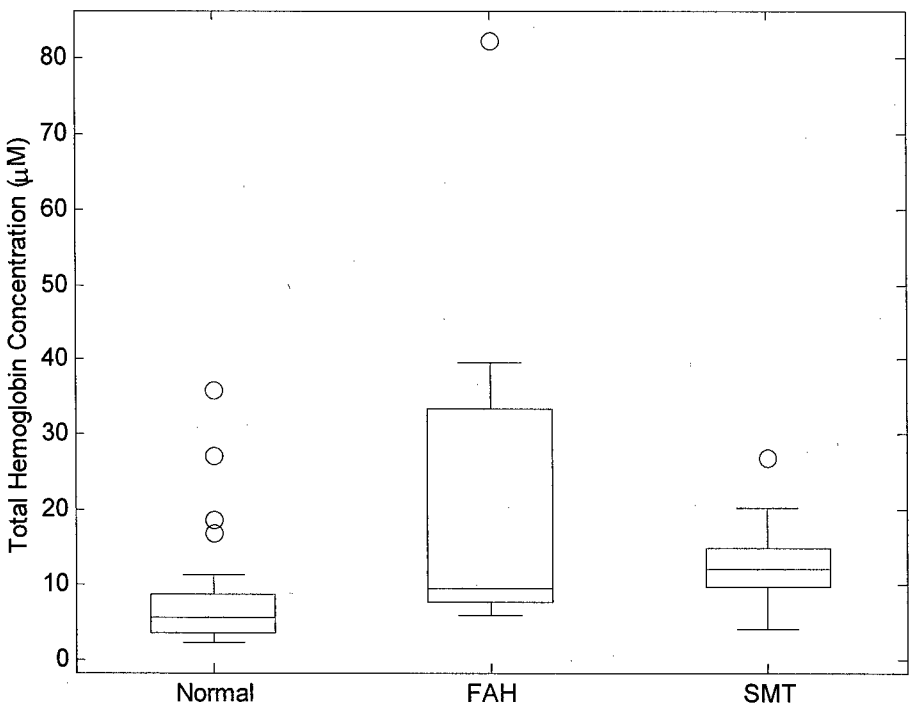
Total Hemoglobin Concentration (μM)
0
10
20
30
40
50
60
70
80
Normal
FAH
SMT

Figure 5 (b)

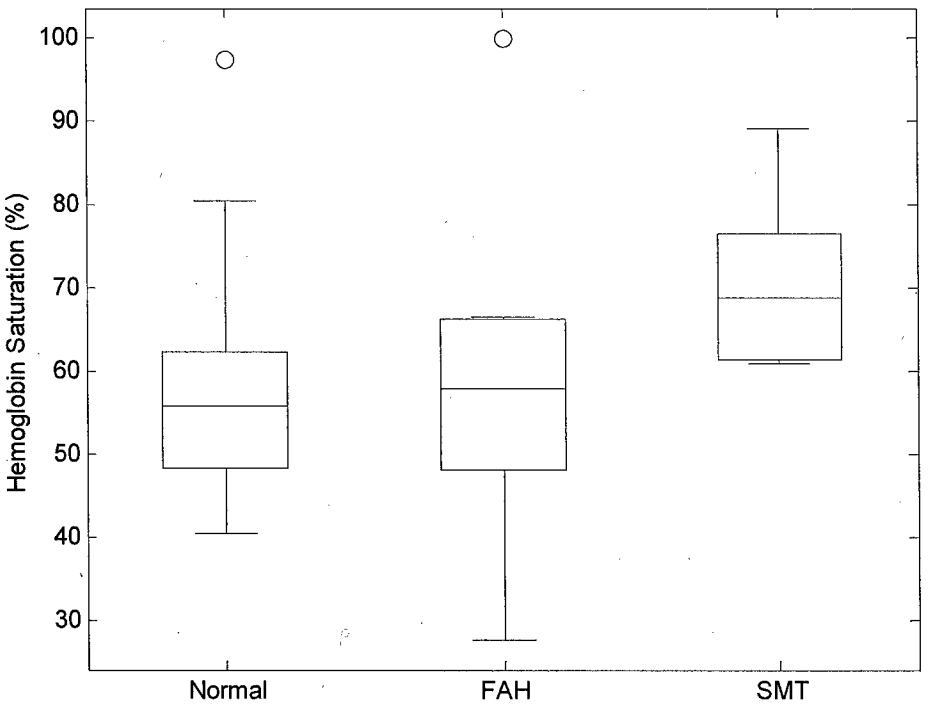

Figure 5 (c)